Supercritical carbon dioxide–activated copper/bacterial cellulose aerogels for the capture of hydrophobic organic liquids

Downloaded from: https://research.chalmers.se, 2024-11-19 04:16 UTC

Citation for the original published paper (version of record):
Le, H., Tran, K., Nguyen, H. et al (2024). Supercritical carbon dioxide–activated copper/bacterial cellulose aerogels for the capture of
hydrophobic organic liquids. Journal of Chemical Research, 48(5).
http://dx.doi.org/10.1177/17475198241280447

N.B. When citing this work, cite the original published paper.

research.chalmers.se offers the possibility of retrieving research publications produced at Chalmers University of Technology. It covers all kind of research output: articles, dissertations, conference papers, reports etc. since 2004. research.chalmers.se is administrated and maintained by Chalmers Library

(article starts on next page)

Check for updates

Research Paper

Journal of Chemical Research

Journal of Chemical Research
September-October 1–11
© The Author(s) 2024
Article reuse guidelines:
sagepub.com/journals-permissions
DOI: 10.1177/17475198241280447
journals.sagepub.com/home/chl
Sage

Supercritical carbon dioxide–activated copper/bacterial cellulose aerogels for the capture of hydrophobic organic liquids

Ha V Le[1,2], Khoa D Tran[1,2], Hanh HM Nguyen[1,2], Kiet TA Nguyen[1,2], Ha T Bui[1,2], Trang TP Nguyen[1,2], Phuoc H Ho[3] and Khoa D Nguyen[1,2]

Abstract

In this study, bacterial cellulose was derived from coconut water via fermentative production of *nata de coco*, a common food in Southeast Asia. Bacterial cellulose offers distinct advantages over plant cellulose resources, including three-dimensional structure, high porosity, high cellulose purity, and the absence of required polluting treatments, making it an ideal candidate for the facile preparation of various functional aerogel materials. Surface modification of *nata de coco*-derived cellulose fibers was obtained by incorporating Cu species (approximately 15 wt%) through an aqueous reaction of $Cu(CH_3COO)_2$ with N_2H_4 at room temperature. The Cu-coated bacterial cellulose aerogels were fabricated via supercritical carbon dioxide drying to maintain the natural three-dimensional matrix and subsequently characterized by various techniques confirming high porosity and crystallinity and successful Cu coating onto the cellulose fiber surface. The Cu-containing aerogel showed a significantly improved adsorption uptake for *n*-hexane (12.6 $g g^{-1}$) in comparison with pure bacterial cellulose–based aerogel (3.2 $g g^{-1}$). Furthermore, notable adsorption performances of 13.6–19.9 $g g^{-1}$ were found for cyclohexane, ethyl acetate, and soybean oil, indicating the high efficiency of the supercritical carbon dioxide–activated bacterial cellulose aerogel containing Cu species in the adsorption of water-insoluble liquids. Notably, applying supercritical carbon dioxide drying afforded the stable aerogel structure for reusing over several cycles with almost unchanged trapping capacity.

Keywords

aerogel, bacterial cellulose, Cu coating, hydrophobic liquid, $scCO_2$ drying

Date received: 18 April 2024; accepted: 13 August 2024

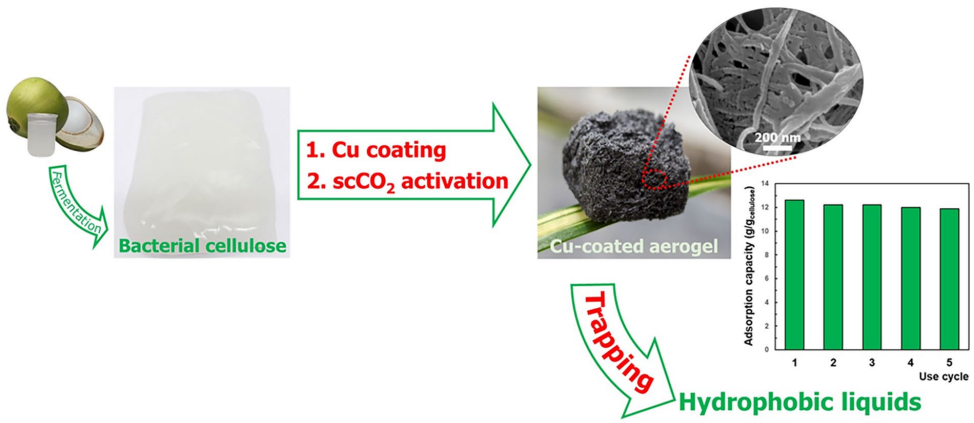

[1]Faculty of Chemical Engineering, Ho Chi Minh City University of Technology (HCMUT), Ho Chi Minh City, Vietnam
[2]Vietnam National University, Ho Chi Minh City, Linh Trung Ward, Thu Duc City, Vietnam
[3]Competence Centre for Catalysis, Chemical Engineering, Chalmers University of Technology, Gothenburg, Sweden

Corresponding authors:
Phuoc H Ho, Competence Centre for Catalysis, Chemical Engineering, Chalmers University of Technology, SE-412 96 Gothenburg, Sweden.
Email: phuoc@chalmers.se

Khoa D Nguyen, Faculty of Chemical Engineering, Ho Chi Minh City University of Technology (HCMUT), 268 Ly Thuong Kiet Street, District 10, Ho Chi Minh City 740500, Vietnam.
Email: khoand1989@hcmut.edu.vn

Creative Commons CC BY: This article is distributed under the terms of the Creative Commons Attribution 4.0 License (https://creativecommons.org/licenses/by/4.0/) which permits any use, reproduction and distribution of the work without further permission provided the original work is attributed as specified on the SAGE and Open Access pages (https://us.sagepub.com/en-us/nam/open-access-at-sage).

Introduction

Non-polar organic solvents are commonly applied to extract and dissolve other organic compounds in various scientific and industrial sectors such as chemical synthesis, manufacture of fuels, lubricants, medicines, paints, polymers, and agricultural products.[1,2] However, the extensive use of non-polar organic solvents has resulted in pollution of water, soil, and air, thereby causing numerous negative effects on both human health and the natural ecosystem. Consequently, wastewater treatment processes require complicated and costly facilities to effectively remove these solvents.[3–5] In addition, the cleanup of oil spills, which have released a large amount of liquid petroleum hydrocarbons into the environment, poses a grand challenge, particularly in marine ecosystems.[6,7] Among available treatment methods, physical adsorption of non-polar solvents has proved to be a rapid, efficient, practical, and environmentally benign approach. Therefore, there is a critical need to develop novel adsorption materials with advanced properties such as advanced hydrophobicity and biodegradability toward improved performance and environmental friendliness.[8–10]

Aerogels have attracted increasing attention from researchers due to unique properties including large specific surface area (up to 1600 $m^2 g^{-1}$), low-to-extremely low density (0.003–0.5 g/cm^3), high porosity (80%–99.8%), and facile textural adjustment. Numerous fields such as optoelectronics, adsorption, catalysis, sound insulation, medical materials, and aerospace materials have benefited from significant achievements in the preparation, improvement, and modification of aerogel materials.[11–13] From environmental and economic perspectives, aerogels derived from biodegradable, inexpensive, and non-toxic polymers are highly desirable. Cellulose, being one of the most plentiful natural polymers, has emerged as a promising candidate for the manufacture of aerogel.[14,15] The adsorption performance of aerogels for hydrophobic solvents generally depends not only on the density and porosity but also on the hydrophobicity and capillary effect. Therefore, to improve the hydrophobicity of the cellulose surface, reagents such as silanes, phosphoric acids, and carboxylates containing alkyl or fluoro groups are commonly applied for surface functionalization despite their high cost and environmental toxicity.[15–20] Alternatively, previous studies have demonstrated that Cu clusters formed on cellulose fibers via a cost-effective and simple reduction by hydrazine at room temperature, followed by freeze-drying, can yield highly hydrophobic aerogel materials.[21,22]

It should be noted that the isolation and purification of cellulose fibers from plants for aerogel preparation usually involve steps requiring toxic chemicals to remove lignin, pectin, and hemicellulose, which often inhibit the formation of the aerogel structure. In addition, energy-intensive processes are generally required to transform rigid linear plant cellulose bundles into a porous matrix.[23–25] In contrast, bacterial cellulose (BC) obtained via the fermentation of biomass sources containing carbohydrates offers significant advantages for the preparation of various functionalized aerogels. These advantages include a non-ordered three-dimensional (3D) structure, high porosity, and high cellulose purity without complicated chemical treatments.[26–30] In tropical regions, for example, Vietnam, coconut water is usually utilized to produce a natural hydrogel form of BC known as *nata de coco*. This product is not only a popular low-calorie food but also serves as an attractive source of BC to fabricate advanced materials applied in water treatment, cosmetics, biomedical, paper, electronic, and textile industries.[31–34] We have recently reported promising and efficient performances of the *nata de coco*-derived BC aerogels, generated via freeze-drying, for the adsorption of organic solvents and the removal of organic dyes from water. The manufacture and modification of the aerogel from *nata de coco* were simpler and less costly as compared to the plant cellulose-base procedure due to the natural 3D network of high-quality BC in this abundant resource.[21,35,36] Besides freeze-drying, supercritical fluid-based activation has been widely utilized to produce aerogels via dissolving the solvents in the supercritical fluids. Supercritical carbon dioxide ($scCO_2$) is the most common agent in this procedure due to its abundance, non-toxicity, non-flammability, thermodynamic stability, and facile adjustment of its physical properties.[37–39] The porous structure of the $scCO_2$-activated aerogel remains preserved to a high level as the disadvantages of conventional drying processes, in which surface tension effects at the vapor–liquid interfaces can lead to structural collapse, generally disappear in $scCO_2$ drying.[37,39,40] Therefore, as a continuation of the development of hydrophobic Cu-including aerogel materials via various drying pathways, this study focuses on *nata de coco*-based BC coated with Cu species using a benign hydrazine reduction procedure that was activated with supercritical CO_2 ($scCO_2$) drying to obtain recyclable aerogels for trapping oleophilic liquids.

Materials and methods

Materials

Copper(II) acetate monohydrate ($Cu(CH_3COO)_2.H_2O$), hydrazine hydrate ($N_2H_4.H_2O$), *n*-hexane, ethyl acetate, and cyclohexane were obtained from Sigma-Aldrich. Soybean oil was purchased from Calofic Corporation. Coconut water was obtained from coconuts (8-month-old) in Ben Tre (Vietnam) and used for the fermentation process by Acetobacter xylinum for 2 weeks, to yield raw *nata de coco* (a brown gelatinous form). Purification and decolorization of *nata de coco* were conducted by immersing in an NaOH solution (1 M) for 24 h and subsequently washing with water until neutralization, resulting in translucent white *nata de coco* in which BC occupied 0.8 wt%.

Preparation of $scCO_2$-activated Cu/BC aerogels

In a typical Cu modification experiment, according to the previous procedure, purified *nata de coco* (125 g, involving approximately 1 g of BC) cut into 1-cm cubic pieces was ground with 75 g of water using a Philips blender (model HR1600, 550 W) for 2 min to obtain a uniform *nata de coco* suspension.[21,41] This suspension was then added to a

Table 1. Detailed preparation of the $scCO_2$-activated BC aerogel samples in this work.

Sample	BC mass (g)	Cu (II) acetate amount (mmol)	N_2H_4 amount (equiv.)	Cu content (wt%)*
Cel	1.0	0	0	0
Hyd-Cel	1.0	0	13	0
Cu-Cel-13	1.0	4.0	13	14.5 ± 0.2
Cu-Cel-26	1.0	4.0	26	14.8 ± 0.1
Cu-Cel-39	1.0	4.0	39	15.2 ± 0.2
Cu-Cel-52	1.0	4.0	52	15.0 ± 0.3

*Determined by inductively coupled plasma-optical emission spectrometry measurement (ICP-OES).

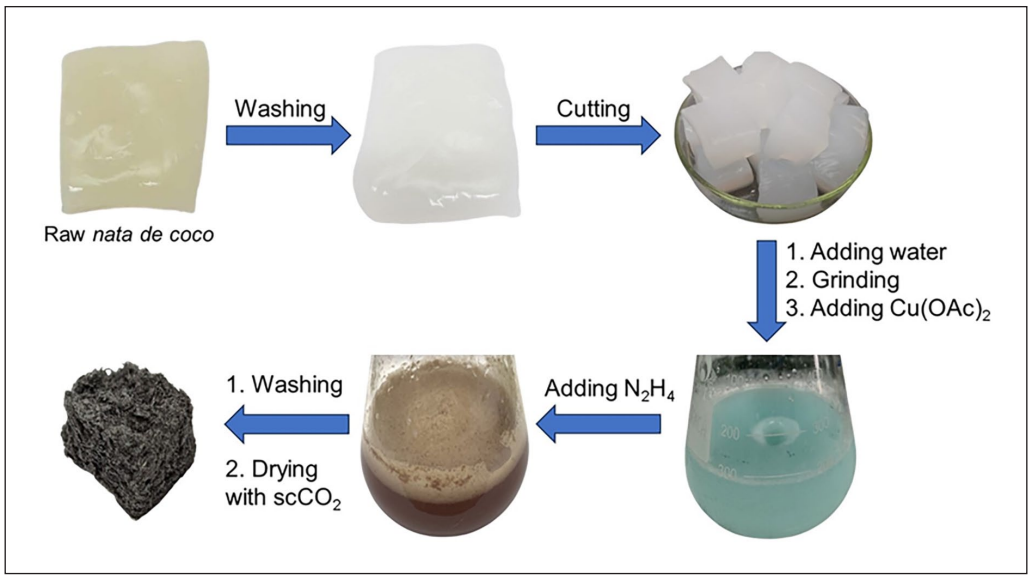

Figure 1. Procedure of the preparation of $scCO_2$-activated Cu/BC aerogels from *nata de coco*.

500-mL Erlenmeyer flask containing copper(II) acetate hydrate (4.0 mmol, 0.741 g), followed by vigorous stirring for 1 h. Subsequently, hydrazine hydrate (52 equiv., 3.2 mL) was slowly added to the mixture to initiate the reduction of Cu^{2+}-to-Cu^0. After a 12-h reaction at room temperature, the Cu-containing solid was collected *via* filtration, washed with water, and then subjected to five exchanges with absolute ethanol. The material was then dried under $scCO_2$ conditions (at 45 °C and 100 bar for 6 h), resulting in the formation of the Cu-modified cellulose aerogel denoted as Cu-Cel-52, in which "52" indicates the number of hydrazine equivalents compared to the Cu(II) salt used. For comparison purposes, similar experiments were carried out in the absence of copper(II) acetate (yielding the aerogel sample denoted as Hyd-cel) and in the absence of both the Cu(II) precursor and hydrazine (yielding the aerogel sample denoted as Cel) (Table 1). The entire modification procedure is summarized in Figure 1.

Characterization of the as-synthesized aerogels

Crystallinity and composition of the materials were investigated by X-ray diffraction (XRD) analysis with Cu-Kα radiation on a Bruker Diffractometer (Model D8 Advance, Germany). The diffraction patterns were recorded at 2θ from 10° to 80° (0.01°/step and 0.6° min^{-1}).

Thermal behaviors of the materials were studied by thermogravimetric analysis (TGA) using a TA Instruments Thermal Gravimetric Analyzer (Model SDT-Q600, New Castle, DE, USA), in which, the sample (~0.01 g) in an alumina crucible was heated from 40 to 900 °C (10 °C min^{-1}) under an air atmosphere. Textural characteristics of the materials were analyzed by nitrogen adsorption/desorption at −196 °C on Micromeritics equipment (Model ASAP 2020, Norcross, GA, USA). Before each sorption experiment, the sample was reactivated at room temperature under vacuum for 12 h.

Morphology of the materials was observed on a Hitachi scanning electron microscope (SEM, Model TM 4000, Japan) connected with an energy-dispersive X-ray spectroscopy (EDX) detector. Fourier-transform infrared spectroscopy (FT-IR) analysis was conducted on a Bruker spectrometer (Model Vertex 70v, Germany) using attenuated total reflectance (ATR) sampling methodology. Each measurement was performed with an accumulation of 32 scans recorded in the wavenumber range of 4000–400 cm^{-1} at a resolution of 4 cm^{-1}.

Adsorption studies

In a typical experiment of *n*-hexane adsorption, an aerogel sample with the predetermined mass ($m_{cellulose}$, g) was added to a 50-mL glass bottle containing *n*-hexane (m_1, g) (Figure

S1 in Supporting Information). After a predetermined period, the sample was gently taken from the liquid. Until no free *n*-hexane drops were observed, the total mass (m_2, g) of the bottle involving *n*-hexane was recorded. The adsorption capacity of the aerogel for *n*-hexane (Q, $g_{n\text{-}hexane}/g_{cellulose}$) was determined based on equation (1)

$$Q = \frac{m_1 - m_2}{m_{sample}} \quad (1)$$

The effect of the experiment conditions on the adsorption efficiency was investigated, including the drying method (thermal drying and $scCO_2$ drying) to obtain the Cu-containing aerogel, the Cu presence in the aerogel, the N_2H_4 amount used in the Cu^{2+}-to-Cu^0 reduction (13–52 equiv.), and the adsorption time (0–300 s). Furthermore, the Cu/BC aerogel was applied to adsorb other hydrophobic organic liquids including cyclohexane, ethyl acetate, and soybean oil. Each adsorption experiment was performed three times.

The experimental data of the time-dependent adsorption capacity of Cu-Cel-52 for soybean oil were applied to first-order and second-order kinetic models (equations (2) and (3), respectively) to discover the adsorption kinetics[42]

$$ln(Q_e - Q_t) = lnQ_e - k_1 t \quad (2)$$

$$\frac{t}{Q_t} = \frac{1}{k_2 Q_e^2} + \frac{1}{Q_e} t \quad (3)$$

in which Q_e ($g_{oil}/g_{aerogel}$) is the adsorption capacity at the equilibrium, Q_t ($g_{oil}/g_{aerogel}$) is the adsorption capacity at a given interval t (min), and k_1 (min^{-1}) and k_2 ($g_{aerogel}\ g_{oil}^{-1}\ min^{-1}$) are the rate constants of first- and second-order adsorption model.

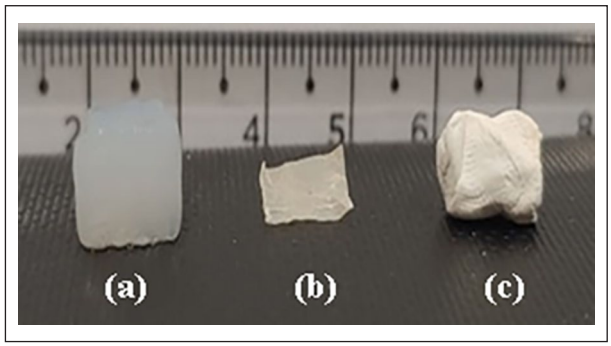

Figure 2. (a) Raw *nata de coco* sample, (b) *nata de coco* after thermal drying, and (c) *nata de coco* after $scCO_2$ drying. The unit of the ruler is a centimeter.

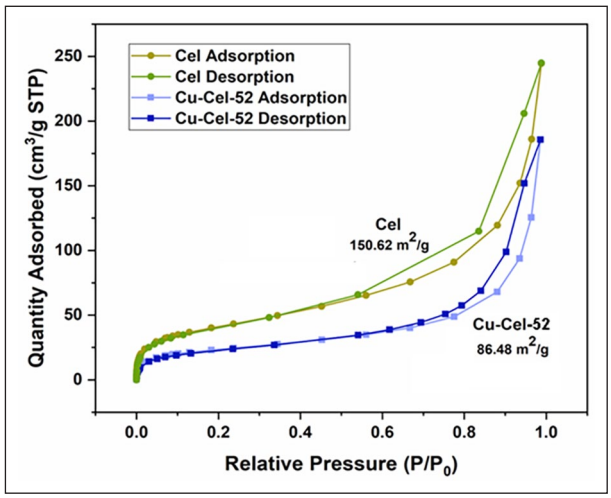

Figure 3. N_2 sorption isotherms for the aerogel of fresh BC (Cel) and the aerogel of Cu-coated BC (Cu-Cel-52).

Results and discussion

Characterization of $scCO_2$-activated Cu/BC aerogels

BC in *nata de coco* possesses a three-dimensional matrix due to the random arrangement of *Acetobacter xylinum* during the fermentation and production of the cellulose fibers (Figure 2(a)). However, conventional thermal drying of *nata de coco* at 120 °C under normal atmospheric conditions resulted in the formation of hard cellulose sheets lacking porosity (Figure 2(b)). To preserve the porous cellulose structure, $scCO_2$ drying was applied to prevent structural collapse during the removal of solvents, for example, ethanol used in the washing step. Consequently, the obtained product exhibited aerogel-like properties with a size similar to that of the original *nata de coco* samples. Moreover, the cellulose aerogel had softness and lightweight characteristics, making it promising for further modification with Cu (Figure 2(c)). Surface modification of BC fibers with the Cu species was achieved through the reaction of the Cu^{2+} cations with hydrazine to form Cu(0) at ambient conditions in the *nata de coco* suspension, as previously described.[41] As shown in Figure 1, upon the addition of hydrazine hydrate, the mixture color changed from blue to yellow and eventually to reddish brown, indicating the formation of Cu(0) in the suspension. Following $scCO_2$ drying, the resulting aerogel retained almost the same size as the pristine *nata de coco* piece, ready for subsequent adsorption studies.

To gain a comprehensive understanding of the pore texture, nitrogen sorption at 77 K was employed to determine surface areas, pore volumes, and pore size distribution. Specifically, the sorption behavior of cellulose aerogel and Cu-modified materials showed typical type IV isotherms with a hysteresis loop (Figure 3), which was assigned for the presence of a pore system with various pore diameters from meso- to macro-scale sizes.[43–45] The $scCO_2$ drying proved to be an efficient method to remove solvent molecules while preserving the 3D BC network. Moreover, the Cu-modified material exhibited a significant decrease of approximately 40% in N_2 uptake compared to the pristine aerogel. The BET surface area and pore volume of Cu-loaded material were determined to be approximately 86 and 0.28 $cm^3\ g^{-1}$, respectively, while these values of the fresh aerogel were approximately 150 and 0.37 $cm^3\ g^{-1}$, respectively. These decreases in the porosity were likely attributed to the incorporation of Cu species into the framework, which hindered gas phase diffusion, and thereby inhibited the nitrogen uptake by the cellulose matrix.[41]

To further confirm the presence of Cu in the aerogel, TGA was performed in air from 25 to 900 °C. In the TGA

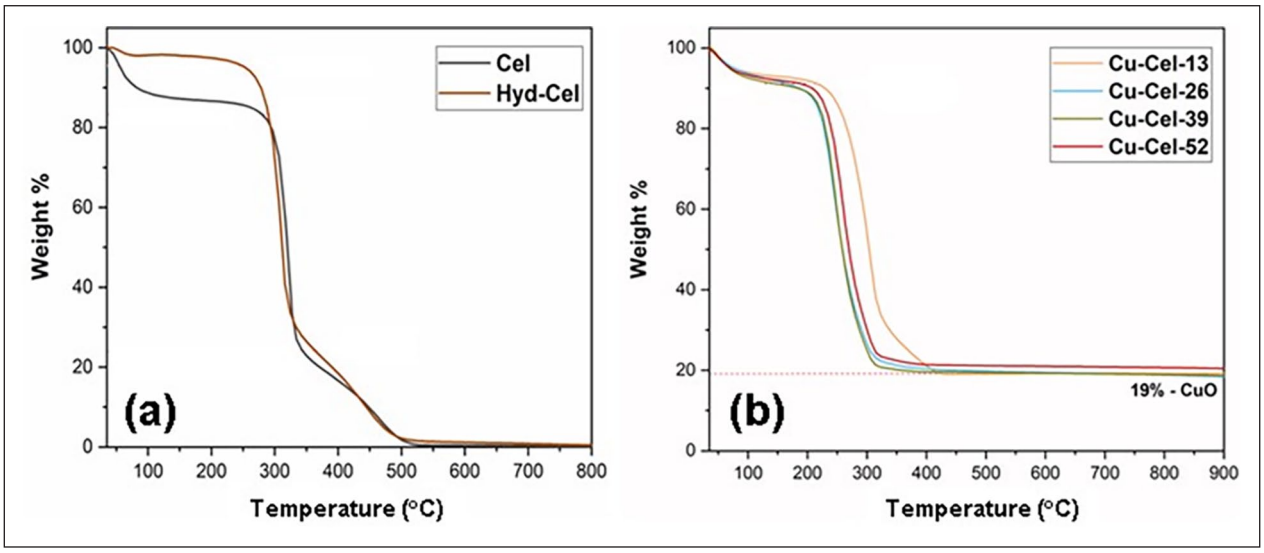

Figure 4. TGA profiles of (a) Cu-free aerogels and (b) Cu-containing aerogels.

profile of the unmodified aerogel material (Figure 4(a)), the material was stable up to 300 °C and its mass rapidly decreased at the higher temperature region. This can be rationalized by the thermal decomposition of cellulose, wherein the carbohydrate chain was broken and combusted, ultimately resulting in carbon oxides and water as final oxidized products.[46] In contrast, the remaining mass of the Cu-loaded samples (Figure 4(b)) ranged from 19 to 21 wt% after the thermal degradation, indicating the formation of CuO as the sole solid phase. Based on these CuO amounts, it was determined that Cu contents accounted for 15 to 16 wt% in the modified aerogel samples. In addition, the inductively coupled plasma (ICP) analysis also revealed Cu contents of 14.6–15.2 wt% for the Cu-containing aerogels, 30% lower than the $Cu(OAc)_2$-based theoretical value of approximately 20 wt%, which can be rationalized by incomplete reduction and coating as well as Cu losses during the washing and filtration steps.

The XRD measurements were carried out to identify crystalline phases present in the BC-based aerogels. According to the XRD patterns (Figure 5), the materials derived from BC were highly crystalline. Specifically, two typical and intense peaks corresponding to crystalline cellulose were observed at $2\theta = 14.5°$ and 22.7° in all of the XRD profiles. Furthermore, the successful loading of Cu species in the Cu/BC aerogels was confirmed by the appearance of three additional peaks at $2\theta = 43.8°$, 51.5°, and 74.2°, which were assigned to the (111), (200), and (222) planes of the Cu^0 phase, respectively.[47] Moreover, the modification process had no significant effect on the cellulose structure as evidenced by the maintenance of characteristic peaks of crystalline cellulose with high intensity. This result is consistent with the findings of Li et al.[41] regarding the modification of plant cellulose with Cu species. On the contrary, the aerogel samples prepared using 13 and 26 equiv. of hydrazine, namely, Cu-Cel-13 and Cu-Cel-26, revealed a broad diffraction peak of the CuO phase in their XRD pattern while this peak was not detected for those of Cu-Cel-39 and Cu-Cel-52. The Cu-based products of the

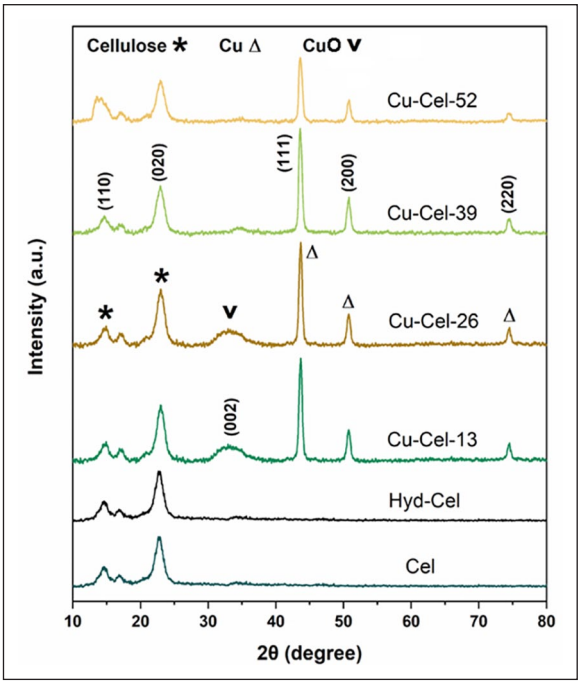

Figure 5. XRD patterns of as-prepared BC-based aerogels.

reduction of the Cu^{2+} cations in the presence of BC depended on the applied hydrazine amount.[48–50] Moreover, as shown in Table 1, the Cu content in the aerogel was improved from 14.5 ± 0.2 to 15.2 ± 0.2 wt% in response to the increase of hydrazine from 13 to 39 equiv., indicating that reduction-based formation and coating of Cu species onto the cellulose surface required a large excess of hydrazine (up to 39 equiv.). In other words, strongly basic conditions ($pH > 11$) should be applied for the Cu modification procedure, in line with the literature.[49,51,52] However, further adding hydrazine into the reaction mixture to 52 equiv. led to a slight reduction in the Cu content to 15.0 ± 0.3 wt%. This can be explained based on the fact that the BC surface can only host a given number of Cu species and when too

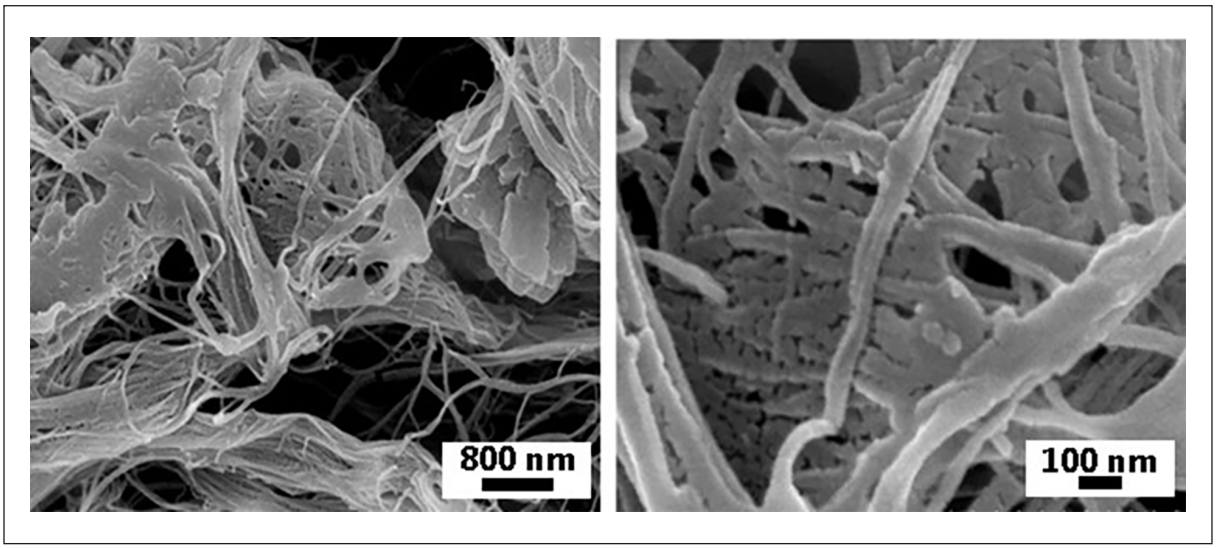

Figure 6. SEM images of the Cu-Cel-52 aerogel sample.

many Cu species were formed during the reduction, only a part of them can be located on the BC surface while the rest would precipitate in the liquid phase.

The morphology of Cu-loaded samples was investigated *via* the SEM measurement. In detail, SEM images of Cu-Cel-52 (Figure 6) revealed the nanoscale structure of surface-modified cellulose material. It can be observed that the diameter of the BC fibers or ribbons was in the range of 40–60 nm, forming a three-dimensional fiber matrix with numerous free spaces. The average pore size of 20 voids observed from the SEM image was approximately 110 ± 60 nm. In addition, the Cu species were found in 40–50 nm clusters on the surface of the cellulose bundles. The fiber diameter was smaller as compared to the size of the Cu cluster; therefore, the formed Cu clusters could easily agglomerate within the matrix. On the contrary, the FT-IR measurement was performed to identify the functional groups present in the BC aerogel and their chemical changes, if any, in the modification procedure (Figure 7). In detail, the FT-IR spectra of the unmodified aerogel (Cel sample) revealed the characteristic bands at the wavenumbers of around 3350, 2850, 1650, and 1100 cm^{-1}, which were assigned to stretching vibrations of the O–H, C–H, C=O, and C–H bonds in cellulose.[21,53–55] *via* No significant differences were detected for the aerogel samples treated with only hydrazine (Hyd-Cel sample) and coated with Cu species (Cu-Cel sample), indicating that the applied reductive conditions and the Cu modification had no chemical impacts on the functional groups of the cellulose chain. Although the presence of the CuO phase in the Cu-Cel-13 and Cu-Cel-26 samples was confirmed the XRD analysis, the signature bands at the wavenumber range of 500–600 cm^{-1} for the Cu–O bond disappeared in their FT-IR spectra probably due to the low content of CuO under the detection limit of FT-IR.[56,57]

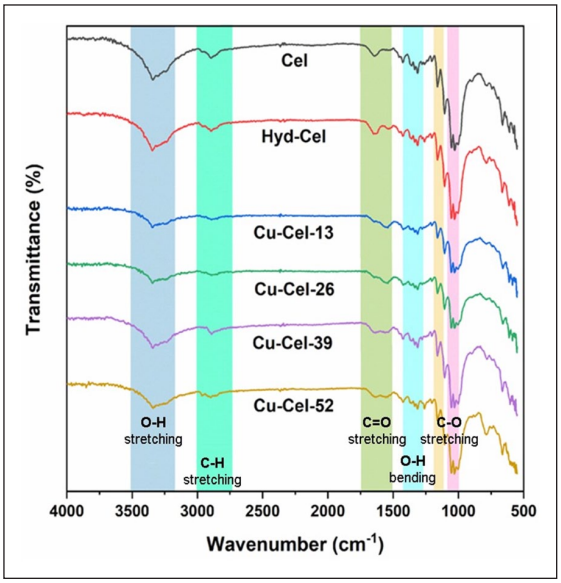

Figure 7. FT-IR results of as-prepared bacterial cellulose-based aerogels.

Adsorption studies

Cellulose aerogel is anticipated to trap various solvents because it not only contains a lot of hydrophilic hydroxyl groups but also possesses a porous structure.[58] However, employing unmodified materials derived from cellulose for adsorbing non-polar organic solvents is not particularly effective due to the abundant presence of polar groups (–OH groups) on its backbone. To improve the non-polar liquid adsorption capacity of cellulose-based materials, covering or blocking hydroxyl groups with metal nanoparticles is an effective approach. This increases the hydrophobicity of cellulose fiber surfaces and significantly improves the affinity for non-polar organic molecules. Besides, the surface tension of non-polar organic compounds is usually lower than that of polar chemicals. For example, the surface tension of *n*-hexane is 18.43 mN m^{-1} at 20 °C, which is four times lower than water at the same condition (72.3 mN m^{-1}).[59] This offers a good opportunity for non-polar solvents to penetrate the Cu layer because of the good interaction.[7,41,60]

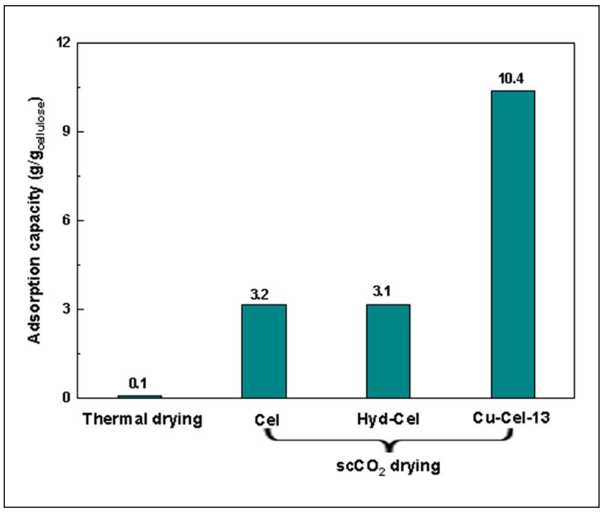

Figure 8. Effect of drying methods and the modification with Cu on trapping *n*-hexane (trapping conditions: adsorbent 0.02 g, contact time 300 s).

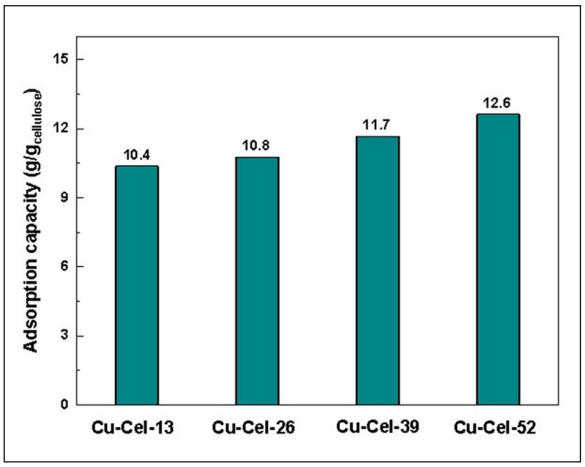

Figure 9. Effect of the hydrazine amount used for the Cu^{2+}-to-Cu^0 reduction on the *n*-hexane adsorption (coating conditions: *nata de coco* 125 g, water 75 g, grinding time 2 min, $Cu(Oac)_2$ 4.0 mmol, N_2H_4 13–52 equiv., reaction time 12 h; trapping conditions: aerogel 0.02 g, contact time 300 s).

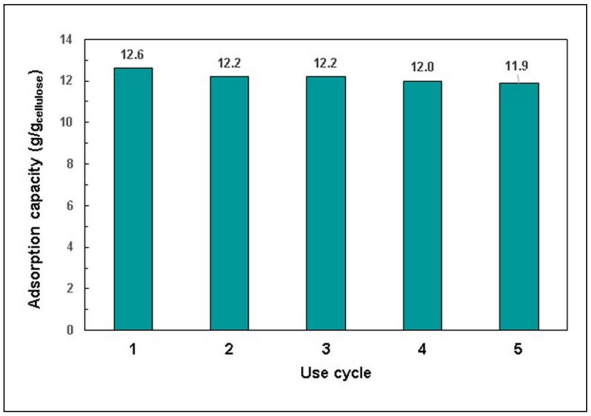

Figure 10. Recycling studies for Cu-Cel-52 in the *n*-hexane adsorption (trapping conditions: Cu-Cel-52 0.02 g, contact time 300 s).

In this work, a series of experiments were conducted using different samples of BC aerogel to capture *n*-hexane under ambient conditions to investigate the effect of Cu nanoparticles presence on the surface of cellulose fibers. The results in Figure 8 demonstrated the important role of cellulose surface modification as well as the activation method. Particularly, the adsorption capacities of aerogel materials prepared by $scCO_2$ drying were recorded to be about 3.0 g g^{-1}, whereas almost no adsorption of *n*-hexane was observed when using BC obtained from *nata de coco* via thermal activation. No difference in the activity was observed for the sample treated with only hydrazine, indicating that hydrazine did not affect the adsorption properties of the aerogel. Importantly, the *n*-hexane trapping capacity of the Cu-modified material was significantly increased from 3.1 to 10.4 g g^{-1}. This suggests that the presence of Cu species indeed enhanced the hydrophobicity of the cellulose fiber surface, thereby improving the *n*-hexane adsorption capacity.

As above described, the presence of the Cu-based phases in the aerogel was affected by the used hydrazine. Therefore, the quantity of hydrazine also played an important role in adsorbing *n*-hexane. In particular, a higher molar ratio of N_2H_4/Cu^{2+} led to a higher adsorption capacity was recorded. The best capacity of 12.6 g/g was obtained for the Cu-loaded aerogel prepared with 52 equiv. of hydrazine (Figure 9). When a smaller amount of hydrazine was utilized, the formed Cu species were insufficient to block all of the hydroxyl groups on the cellulose surface, thereby hindering the adsorption of *n*-hexane. The presence of the unreduced CuO phase in the XRD patterns might strengthen this explanation. Therefore, it is necessary to cover the cellulose aerogel surface with Cu species and prevent the unexpected oxidation of Cu species to other phases. With the best performance, the Cu-Cel-52 was applied for the next studies.

After the *n*-hexane trapping experiment, *n*-hexane was easily removed from the spent Cu-Cel-52 aerogel at room temperature under atmospheric pressure due to its low boiling point. The recovered aerogel was subsequently applied to the next trapping cycle without any further reactivation. As shown in Figure 10, only minor decreases (<6%) in the capacity of Cu-Cel-52 in capturing *n*-hexane were observed in several recycling cycles. At the fifth use, Cu-Cel-52 can adsorb *n*-hexane 11.9 times its mass, indicating the high stability of the porous network in the aerogel. The SEM images of the spent sample (Figure S2 in Supporting Information) showed a non-ordered matrix of the Cu-coated BC bundles, generating a large number of pores with different sizes (130 ± 34 nm), similar to the pristine one. It can be concluded that the collapse of the aerogel structure was negligible during trapping and eliminating *n*-hexane due to the complicated BC network which was probably strengthened by coating Cu.

To demonstrate the trapping efficiency of the $scCO_2$-dried Cu/BC aerogel, other water-insoluble organic liquids, including cyclohexane, ethyl acetate, and soybean oil, were employed for the adsorption experiment (Figure S1 in Supporting Information). The liquid-trapping capacity of the $scCO_2$-dried Cu/BC aerogel was directly proportional

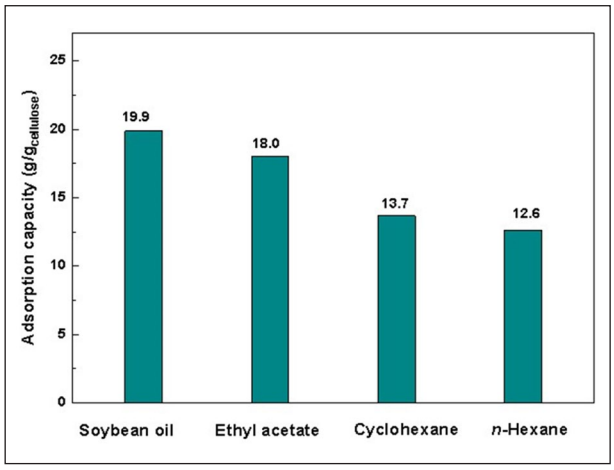

Figure 11. Trapping capacity of the Cu-Cel-52 aerogel for different hydrophobic solvents (trapping conditions: Cu-Cel-52 0.02 g, contact time 300 s).

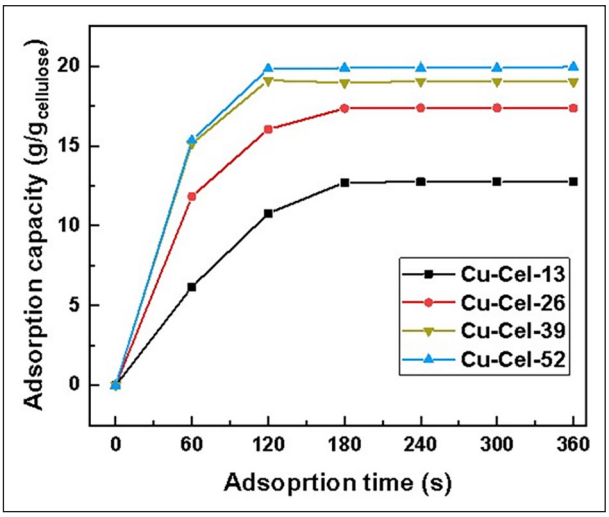

Figure 12. Effect of the contact time on trapping soybean oil (trapping conditions: Cu-Cel-52 0.02 g, contact time 0–300 s).

to the density of the applied liquids (Figure 11). Indeed, a gram of Cu-Cel-52 could adsorb 19.9 g of soybean oil (d = 0.92 g mL^{-1}), while the uptake of *n*-hexane (d = 0.66 g mL^{-1}) was recorded at 12.6 g g^{-1}. In other words, more mass of a denser solvent can be captured in the identical pore volume in the aerogel network, in line with the trend given for the oil-trapping materials.[41,61,62] Based on these obtained trapping results, if the adsorption performance is presented in the mL g^{-1} unit, the total volumetric trapping capacities of the Cu-Cel-52 aerogel for the water-immiscible liquids could be determined to be around 20 mL g^{-1}. These volumetric values were higher than those previously reported for the hydrophobic silica aerogel (16 mL g^{-1}).[32]

Soybean oil with the highest viscosity among the tested organic liquids, similar to crude oil, was further employed to investigate the effect of the contact time on the adsorption capacity of various Cu-loaded aerogels. Generally, the time-dependent adsorption curves of soybean oil into aerogels showed a similar trend, wherein the capture efficiency rapidly increased in the first 120 s, then gradually slowed down before reaching a plateau at 180 s. Similar to the results obtained with *n*-hexane, as shown in Figure 12, only 12.5 g g^{-1} of soybean oil could be adsorbed when Cu-Cel-13 was used. The best performance of about 20 g g^{-1} was observed for Cu-Cel-52, highlighting the importance of the complete reduction of Cu(II) into Cu(0) for modifying the BC surface in the aerogel. These trapping results were used to describe the trapping kinetics *via* the pseudo-first-order and second-order models. The determination coefficients (R^2) of the pseudo-first-order model of trapping soybean oil by the Cu-coated aerogels were found to be from 0.40 to 0.67 while using the pseudo-second-order model gave much better R^2 values (0.97–0.99) (Figure S3 in Supporting Information). On the contrary, the equilibrium oil uptakes for the samples calculated from the pseudo-second-order model were very close to the experimental data (Table S1 in Supporting Information). Therefore, the capture of soybean oil into all of the aerogels was well fitted to the pseudo-second-order model. In fact, according to Wang et al.,[32] the mechanism of capturing organic liquids into the aerogel was simply suggested to be based on the viscous liquid flow that inhaled the porous matrix of the aerogel due to the capillary force.

The adsorption performance of modified BC aerogel (Cu-Cel-52) was compared to those of several other adsorbents, which were previously reported (Table 2).[61–64] To be more specific, the removal efficiency of Cu-modified aerogel for *n*-hexane and cyclohexane in this work was 12.6 and 13.6 g g^{-1}, respectively, while Meng et al.[63] reported values of approximately 7.0 g g^{-1} using an aerogel composite derived from cellulose and chitosan (Entry 2). In the study by Ghorbal et al., a simple method to produce a new and eco-friendly composite cryogel combined with keratin and cellulose was introduced.[61] The prepared material was fully characterized and then employed to remove various organic solvents with adsorption capacities from 6.9 to 17.7 g g^{-1}.[61] However, the trapping efficiency of *n*-hexane and vegetable oil was recorded at 7.1 and 8.3 g g^{-1},[61] respectively,

Table 2. Hydrophobic liquid-trapping capacity of cellulose-based materials.

Cellulose-based materials	*n*-Hexane (d = 0.66 g mL^{-1})	Cyclohexane (d = 0.77 g mL^{-1})	Soybean oil/vegetable oil (d = 0.91–0.93 g mL^{-1})	Reference
Cellulose/chitosan composite	7.0	6.8	–	Meng et al.[63]
Keratin/cellulose cryogel	7.1	–	8.3	Guiza et al.[61]
Coco peat powder/Fe_3O_4 composite	–	5.1	5.9	Yang et al.[62]
Cellulose-derived carbon nanotube	2.7	–	2.3	Zhang et al.[64]
scCO_2-dried Cu/BC aerogel	12.6	13.6	19.9	This work

which is significantly lower than the performance of Cu-modified aerogel presented in this work. Furthermore, the adsorption ability of other materials derived from cellulose, such as coco peat powder or carbon nanotube, was recently reported; however, they could only trap poor amounts of these organic compounds.[62,64] Along with a facile and simple preparation, the high trapping performance of Cu/BC aerogel provided a great potential solution for removing various organic solvents in the practical conditions.

Conclusion

In conclusion, we implemented a simple and efficient method for fabricating Cu-containing BC aerogel derived from *nata de coco* with enhanced trapping capacities for hydrophobic organic solvents using the $scCO_2$ drying technique. The fabrication involved reductively coating Cu onto the BC fibers, followed by the $scCO_2$-based activation, which allowed the BC framework to preserve its pristine complicated 3D structure. The extensive characterizations confirmed the significant benefits of $scCO_2$ drying in the aerogel preparation and the presence of Cu species on the surface of BC fibers and bundles, elucidating its role in trapping hydrophobic organic molecules. Possessing a highly porous matrix with a hydrophobic surface, the Cu-loaded aerogel exhibited impressive capture capacities for various organic chemicals, including *n*-hexane, cyclohexane, ethyl acetate, and soybean oil in a range from 12.6 to 19.9 $g\,g^{-1}$. These results are comparable to or even exceed the performances of previously reported trapping materials derived from cellulose. Importantly, the hydrophobic Cu-containing aerogel showed high textural stability with five successive use cycles for *n*-hexane without significant activity degradation. Based on the promising findings in this contribution, the trapping capacity of the $scCO_2$-activated Cu/BC aerogel for a hydrophobic solvent in both an aqueous solution and an emulsion and the recycling study for non-volatile solvents have been currently under investigation.

Acknowledgements

The authors acknowledge Ho Chi Minh City University of Technology (HCMUT), VNU-HCM for supporting this study.

Author contributions

H.V.L. and P.H.H. contributed to conceptualization. K.D.N. and K.T.A.N. contributed to methodology. K.D.T. and H.H.M.N. contributed to validation. K.T.A.N., H.T.B., and T.T.P.N. contributed to formal analysis. K.T.A.N., H.H.M.N., H.T.B., and T.T.P.N. contributed to investigation. K.D.T. contributed to data curation. H.V.L. contributed to writing—original draft preparation. K.D.N. and P.H.H. contributed to writing—review and editing. H.V.L. and K.D.N. contributed to supervision. All authors have read and agreed to the published version of the manuscript.

Data availability statement

The data presented in this study are available on request from the corresponding author.

Declaration of conflicting interests

The author(s) declared no potential conflicts of interest with respect to the research, authorship, and/or publication of this article.

Funding

The author(s) disclosed receipt of the following financial support for the research, authorship, and/or publication of this article: This research is funded by Vietnam National University HoChiMinh City (VNU-HCM) under grant number: B2024-20-31.

ORCID iD

Phuoc H Ho https://orcid.org/0000-0001-8571-4114

Supplemental material

Supplemental material for this article is available online.

References

1. Clarke CJ, Tu W-C, Levers O, et al. Green and sustainable solvents in chemical processes. *Chem Rev* 2018; 118(2): 747–800.
2. Noel NK, Wenger B, Habisreutinger SN, et al. Utilizing nonpolar organic solvents for the deposition of metal-halide perovskite films and the realization of organic semiconductor/perovskite composite photovoltaics. *ACS Energy Lett* 2022; 7(4): 1246–1254.
3. Karpińska J and Kotowska U. Removal of organic pollution in the water environment. *Water* 2019; 11(10): 2017.
4. Barea E, Montoro C and Navarro JAR. Toxic gas removal—metal–organic frameworks for the capture and degradation of toxic gases and vapours. *Chem Soc Rev* 2014; 43(16): 5419–5430.
5. Woellner M, Hausdorf S, Klein N, et al. Adsorption and detection of hazardous trace gases by metal–organic frameworks. *Adv Mater* 2018; 30(37): 1704679.
6. Dhaka A and Chattopadhyay P. A review on physical remediation techniques for treatment of marine oil spills. *J Environ Manage* 2021; 288: 112428.
7. Haridharan N, Sundar D, Kurrupasamy L, et al. Oil spills adsorption and cleanup by polymeric materials: a review. *Polym Advan Technol* 2022; 33(5): 1353–1384.
8. Pete AJ, Bharti B and Benton MG. Nano-enhanced bioremediation for oil spills: a review. *ACS EST Engg* 2021; 1(6): 928–946.
9. Sayyad Amin J, Vared Abkenar M and Zendehboudi S. Natural sorbent for oil spill cleanup from water surface: environmental implication. *Ind Eng Chem Res* 2015; 54(43): 10615–10621.
10. Adhikari N and Joshi DR. An overview on common organic solvents and their toxicity. *J Pharm Res Int* 2019; 28(3): 1–18.
11. Ateia M, Helbling DE and Dichtel WR. Best practices for evaluating new materials as adsorbents for water treatment. *ACS Mater Lett* 2020; 2(11): 1532–1544.
12. Ganesamoorthy R, Vadivel VK, Kumar R, et al. Aerogels for water treatment: a review. *J Clean Prod* 2021; 329: 129713.
13. Pierre AC and Pajonk GM. Chemistry of aerogels and their applications. *Chem Rev* 2002; 102(11): 4243–4266.
14. Liu Y, Ahmed S, Sameen DE, et al. A review of cellulose and its derivatives in biopolymer-based for food packaging application. *Trends Food Sci Tech* 2021; 112: 532–546.
15. Seddiqi H, Oliaei E, Honarkar H, et al. Cellulose and its derivatives: towards biomedical applications. *Cellulose* 2021; 28(4): 1893–1931.

16. Andou Y, Jeong J-M, Kaneko M, et al. Hydrophobic cellulose fiber surfaces modified with 2,2,3,3,3-pentafluoropropylmethacrylate (FMA) by vapor-phase-assisted photopolymerization. *Polym J* 2010; 42(6): 519–524.
17. Krishnamurthy M, Lobo NP and Samanta D. Improved hydrophobicity of a bacterial cellulose surface: click chemistry in action. *ACS Biomater Sci Eng* 2020; 6(2): 879–888.
18. Guo N, Chen Y, Rao Q, et al. Fabrication of durable hydrophobic cellulose surface from silane-functionalized silica hydrosol via electrochemically assisted deposition. *J Appl Polym Sci* 2015; 132(44): 42733.
19. Etale A, Onyianta AJ, Turner SR, et al. Cellulose: a review of water interactions, applications in composites, and water treatment. *Chem Rev* 2023; 123(5): 2016–2048.
20. Wei DW, Wei H, Gauthier AC, et al. Superhydrophobic modification of cellulose and cotton textiles: methodologies and applications. *J Bioresour Bioprod* 2020; 5(1): 1–15.
21. Nguyen HHM, Tan KVM, Van TTT, et al. Preparation of Cu-modified bacterial cellulose aerogels derived from *nata de coco* towards the enhanced adsorption of hydrophobic organic solvents. *J Porous Mat* 2022; 30: 1195–1205.
22. Nguyen KD, Le THN, Le KTM, et al. Application of *nata de coco* as a biodegradable material for the aqueous adsorption of toxic metal cations. *Mater Today: Proc*. Epub ahead of print 11 March 2023. DOI: 10.1016/j.matpr.2023.02.450.
23. Galiwango E, Abdel Rahman NS, Al-Marzouqi AH, et al. Isolation and characterization of cellulose and α-cellulose from date palm biomass waste. *Heliyon* 2019; 5(12): e02937.
24. Xu D, Fan L, Gao L, et al. Micro-nanostructured polyaniline assembled in cellulose matrix via interfacial polymerization for applications in nerve regeneration. *ACS Appl Mater Interfaces* 2016; 8(27): 17090–17097.
25. Shih Y-T and Zhao Y. Development, characterization and validation of starch based biocomposite films reinforced by cellulose nanofiber as edible muffin liner. *Food Packag Shelf Life* 2021; 28: 100655.
26. Anwar B, Bundjali B and Arcana IM. Isolation of cellulose nanocrystals from bacterial cellulose produced from pineapple peel waste juice as culture medium. *Procedia Chem* 2015; 16: 279–284.
27. Raghav N, Sharma MR and Kennedy JF. Nanocellulose: a mini-review on types and use in drug delivery systems. *Carbohydr Polym Technol Appl* 2021; 2: 100031.
28. Iguchi M, Yamanaka S and Budhiono A. Bacterial cellulose—a masterpiece of nature's arts. *J Mater Sci* 2000; 35(2): 261–270.
29. Fleury B, Abraham E, De La Cruz JA, et al. Aerogel from sustainably grown bacterial cellulose pellicles as a thermally insulative film for building envelopes. *ACS Appl Mater Interfaces* 2020; 12(30): 34115–34121.
30. Chen Y, Zhang L, Yang Y, et al. Recent progress on nanocellulose aerogels: preparation, modification, composite fabrication, applications. *Adv Mater* 2021; 33(11): 2005569.
31. Choi SM, Rao KM, Zo SM, et al. Bacterial cellulose and its applications. *Polymers* 2022; 14(6): 1080.
32. Wang D, McLaughlin E, Pfeffer R, et al. Adsorption of organic compounds in vapor, liquid, and aqueous solution phases on hydrophobic aerogels. *Ind Eng Chem Res* 2011; 50(21): 12177–12185.
33. Onggo D, Mulyani I, Valverde-Muñoz FJ, et al. Bistable thermo-chromic and magnetic spin crossover microcrystals embedded in *nata de coco* bacterial cellulose biofilm. *Cellulose* 2017; 24(5): 2205–2213.
34. Salihu R, Ansari MNM, Abd Razak SI, et al. Catalyst-free crosslinking modification of nata-de-coco-based bacterial cellulose nanofibres using citric acid for biomedical applications. *Polymers* 2021; 13(17): 2966.
35. Phan HT, Nguyen KD, Nguyen HHM, et al. *Nata de coco* as an abundant bacterial cellulose resource to prepare aerogels for the removal of organic dyes in water. *Bioresour Technol Rep* 2023; 24: 101613.
36. Le HV, Dao NT, Bui HT, et al. Bacterial cellulose aerogels derived from pineapple peel waste for the adsorption of dyes. *ACS Omega* 2023; 8(37): 33412–33425.
37. Tomic N, Djekic I, Hofland G, et al. Comparison of supercritical CO_2-drying, freeze-drying and frying on sensory properties of beetroot. *Foods* 2020; 9(9): 1201.
38. Knez Ž, Markočič E, Leitgeb M, et al. Industrial applications of supercritical fluids: a review. *Energy* 2014; 77: 235–243.
39. Benali M and Boumghar Y. Supercritical fluid-assisted drying. In: Mujumdar AS (ed.) *Handbook of industrial drying*. 4th ed. Boca Raton, FL: CRC Press, 2014, pp. 1261–1270.
40. Brown ZK, Fryer PJ, Norton IT, et al. Drying of foods using supercritical carbon dioxide—investigations with carrot. *Innov Food Sci Emerg* 2008; 9(3): 280–289.
41. Li Z, Zhong L, Zhang T, et al. Sustainable, flexible, and superhydrophobic functionalized cellulose aerogel for selective and versatile oil/water separation. *ACS Sustain Chem Eng* 2019; 7(11): 9984–9994.
42. Wang J and Guo X. Adsorption kinetic models: physical meanings, applications, and solving methods. *J Hazard Mater* 2020; 390: 122156.
43. Khalfaoui M, Knani S, Hachicha MA, et al. New theoretical expressions for the five adsorption type isotherms classified by BET based on statistical physics treatment. *J Colloid Interf Sci* 2003; 263(2): 350–356.
44. Howarth AJ, Peters AW, Vermeulen NA, et al. Best practices for the synthesis, activation, and characterization of metal–organic frameworks. *Chem Mater* 2017; 29(1): 26–39.
45. Thommes M. Physical adsorption characterization of nanoporous materials. *Chem Ing Tech* 2010; 82(7): 1059–1073.
46. Yang H, Yan R, Chen H, et al. Characteristics of hemicellulose, cellulose and lignin pyrolysis. *Fuel* 2007; 86(12–13): 1781–1788.
47. Dey G and Elliott SD. Copper reduction and atomic layer deposition by oxidative decomposition of formate by hydrazine. *RSC Adv* 2014; 4(65): 34448–34453.
48. Wang L, Zhang K, Hu Z, et al. Porous CuO nanowires as the anode of rechargeable Na-ion batteries. *Nano Res* 2014; 7(2): 199–208.
49. Medvedeva X, Vidyakina A, Li F, et al. Reductive and coordinative effects of hydrazine in structural transformations of copper hydroxide nanoparticles. *Nanomaterials* 2019; 9(10): 1445.
50. Saikova SV, Vorob'ev SA, Nikolaeva RB, et al. Conditions for the formation of copper nanoparticles by reduction of copper(II) ions with hydrazine hydrate solutions. *Russ J Gen Chem* 2010; 80(6): 1122–1127.
51. Chen JP and Lim LL. Key factors in chemical reduction by hydrazine for recovery of precious metals. *Chemosphere* 2002; 49(4): 363–370.
52. Littrell DM, Bowers DH and Tatarchuk BJ. Hydrazine reduction of transition-metal oxides. *J Chem Soc Farad T 1* 1987; 83(11): 3271–3282.
53. Atykyan N, Revin V and Shutova V. Raman and FT-IR Spectroscopy investigation the cellulose structural differences from bacteria Gluconacetobacter sucrofermentans during the different regimes of cultivation on a molasses media. *AMB Express* 2020; 10(1): 84.

54. Mirmohammadsadegh N, Shakoori M, Moghaddam HN, et al. Wound healing and anti-inflammatory effects of bacterial cellulose coated with *Pistacia atlantica* fruit oil. *Daru* 2022; 30(1): 1–10.
55. Gomes RJ, Ida EI and Spinosa WA. Nutritional supplementation with amino acids on bacterial cellulose production by Komagataeibacter intermedius: effect analysis and application of response surface methodology. *Appl Biochem Biotechnol* 2022; 194(11): 5017–5036.
56. Khalaji AD, Pazhand Z, Kiani K, et al. CuO nanoparticles: preparation, characterization, optical properties, and antibacterial activities. *J Mater Sci: Mater El* 2020; 31(14): 11949–11954.
57. Reddy KR. Green synthesis, morphological and optical studies of CuO nanoparticles. *J Mol Struct* 2017; 1150: 553–557.
58. Hopson C, Villar-Chavero MM, Domínguez JC, et al. Cellulose ionogels, a perspective of the last decade: a review. *Carbohydr Polym* 2021; 274: 118663.
59. Agrawal P, Salomons TT, Chiriac DS, et al. Facile actuation of organic and aqueous droplets on slippery liquid-infused porous surfaces for the application of on-chip polymer synthesis and liquid–liquid extraction. *ACS Appl Mater Interfaces* 2019; 11(31): 28327–28335.
60. Schnell G, Polley C, Bartling S, et al. Effect of chemical solvents on the wetting behavior over time of femtosecond laser structured Ti6Al4V surfaces. *Nanomaterials* 2020; 10(6): 1241.
61. Guiza K, Ben Arfi R, Mougin K, et al. Development of novel and ecological keratin/cellulose-based composites for absorption of oils and organic solvents. *Environ Sci Pollut Res Int* 2021; 28(34): 46655–46668.
62. Yang L, Wang Z, Yang L, et al. Coco peat powder as a source of magnetic sorbent for selective oil–water separation. *Ind Crop Prod* 2017; 101: 1–10.
63. Meng G, Peng H, Wu J, et al. Fabrication of superhydrophobic cellulose/chitosan composite aerogel for oil/water separation. *Fiber Polym* 2017; 18(4): 706–712.
64. Zhang T, Hu F, Zhang C, et al. A novel multi-wall carbon nanotubes/poly(*n*-butylacrylate-co-butyl methacrylate) hybrid resin: synthesis and oil/organic solvents absorption. *Fiber Polym* 2017; 18(10): 1865–1873.